Available online at www.sciencedirect.com
SCIENCE DIRECT®
Journal of Solid State Chemistry 177 (2004) 2101–2114
JOURNAL OF SOLID STATE CHEMISTRY
http://elsevier.com/locate/jssc

Synthesis and characterization of the reduction properties of cobalt-substituted lanthanum orthoferrites

Frank J. Berry,[a] J. Ramón Gancedo,[b] José F. Marco,[b,*] and Xiaolin Ren[a]

[a] *Department of Chemistry, The Open University, Walton Hall, Milton Keynes MK7 6AA, UK*
[b] *Instituto de Química-Física 'Rocasolano', Consejo Superior de Investigaciones Científicas, c/Serrano 119, Madrid 28006, Spain*

Received 10 November 2003; received in revised form 9 February 2004; accepted 15 February 2004

Abstract

Perovskite-related materials of composition $LaFe_{1-x}Co_xO_3$ have been prepared by conventional calcination methods. The temperature programmed reduction profiles indicate that the incorporation of cobalt renders the materials more susceptible to reduction when treated in a flowing mixture of hydrogen and nitrogen. The reduction processes have been examined by ^{57}Fe Mössbauer spectroscopy and Fe K-edge-, Co K-edge- and La L_{III}-edge XANES and EXAFS. The results show that in iron-rich systems the limited reduction of iron and cobalt leads to the segregation of discrete metallic phases without destruction of the perovskite structure at temperatures up to 1200°C. In materials where $x \geqslant$ ca.0.5 the reduction of Co^{3+} to Co^0 precedes complete reduction of Fe^{3+} and the segregation of alloy and metal phases is accompanied by destruction of the perovskite structure.

Keywords: Lanthanum cobalt orthoferrites; Mossbauer; XANES; EXAFS

1. Introduction

Perovskite-related rare earth orthoferrites have attracted interest because of their potential for use as logic- or memory-component devices and as laser and light modulators in optical materials [1,2]. The solids are also catalytically active for hydrocarbon oxidation and for combustion [3] and can be used in sensors [4–6] and solid electrolytes [7–9]. Rare earth orthoferrites, which contain only trivalent metal ions in the structure, are amenable systems for isovalent substitution and systems of the type $LaFe_{1-x}Co_xO_3$ have attracted interest in recent years [10–12] because of their potential for electroceramic and catalytic oxidation application. Such materials have also been recently found to be suitable components in automobile exhaust catalyst systems [13]. In several of these types of applications the materials operate under gaseous reducing conditions and the identification of the nature of the partially reduced phases, which has received little attention in the past, is important if a better understanding of the factors which influence their performance is to be achieved. We have therefore synthesized materials of the type $LaFe_{1-x}Co_xO_3$ and we report here on the characterization of phases formed by treatment in hydrogen.

2. Experimental

Compounds of the type $LaFe_{1-x}Co_xO_3$ were prepared by grinding appropriate quantities of lanthanum(III) oxide, α-iron(III) oxide and cobalt(II) oxide in an agate pestle and mortar and heating in air at 1200°C (12 h). Temperature programmed reduction profiles were recorded from ca. 150 mg samples in flowing 10% hydrogen/ 90% nitrogen (15–20 mL/min) with the temperature being increased by 5°C/min.

X-ray powder diffraction patterns were recorded at 298 K with a Siemens D5000 diffractometer using Cu$K\alpha$ radiation. The lattice parameters were calculated using the program PowerCell for Windows version 2.4 [14].

^{57}Fe Mössbauer spectra were recorded at 298 K with a constant acceleration spectrometer in transmission geometry using a 400 MBq ^{57}Co/Rh source. The drive velocity was calibrated with the ^{57}Co/Rh source and a natural iron foil. All the isomer shift data are reported relative to that of metallic iron at room temperature. The spectra were computer-fitted using the usual constraints of equal width and area for the two lines

*Corresponding author. Fax: +3491-564-2431.
E-mail address: jfmarco@iqfr.csic.es (J.F. Marco).

0022-4596/$ - see front matter © 2004 Elsevier Inc. All rights reserved.
doi:10.1016/j.jssc.2004.02.019

of doublets and equal width and areas in the ratio 3:2:1:1:2:3 for the lines of sextets. In some cases where hyperfine magnetic field distributions were evident, the spectra were fitted to a histogram of sextets without any predetermined shape for the distribution. XANES and EXAFS measurements were performed at Station 8.1 (Fe K-, Co K- and La L-edge) at the Synchrotron Radiation Source at Daresbury Laboratory operating at an energy of 2.0 GeV and an average current of 200 mA. Data were collected at 298 K. The edge profiles were separated from the EXAFS data and, after subtraction of linear pre-edge background, normalized to the edge step. The edge position was defined as the energy at which the first maximum of the first derivative of the absorption edge appears. The energy scale was calibrated using 6 μm iron- and cobalt-foil, and lanthanum oxide. The position of the iron foil edge was taken at 7112.3 eV, that of the cobalt foil edge was at 7708.9 eV, and that of lanthanum oxide, La_2O_3, at 5480.6 eV. All the iron, cobalt and lanthanum XANES data are reported here relative to these values. The EXAFS oscillations were isolated after background subtraction of the raw data using the Daresbury program EXBACK and converted into k space. The data were weighted by k^3, where k is the photoelectron wave vector, to compensate for the diminishing amplitude of EXAFS at high k. The data were fitted using the Daresbury program EXCURV90.

3. Results and discussion

Materials of composition $LaFe_{1-x}Co_xO_3$ ($x = 0$, 0.1, 0.5, 0.9, 1) were shown by X-ray powder diffraction to be single phase. Electron microscopy showed all the particles to have a particle size of ca. 2 μm. The X-ray powder diffraction patterns showed the perovskite-related $LaFe_{1-x}Co_xO_3$ to transform from the orthorhombic $LaFeO_3$- to the hexagonal $LaCoO_3$-type structure between $x = 0.1$ and $x = 0.5$ and are consistent with previous reports [10,11]. The lattice parameters calculated according to the adoption of the orthorhombic or hexagonal unit cell were similar to those reported earlier [11].

3.1. $LaFeO_3$

The temperature programmed reduction (tpr) profile recorded from the compound $LaFeO_3$ (Fig. 1) showed two broad peaks at ca. 500°C and 1200°C. The temperatures at which the peak maxima were observed were sensitive to the gas flow rate and hence all data reported here were recorded at a flow rate of 15–20/min.

The tpr profiles recorded from materials of the type $LaFe_{1-x}Co_xO_3$ (Fig. 1) also showed two peaks albeit at lower reduction temperatures when the cobalt content x was greater than 0.1.

The ^{57}Fe Mössbauer spectrum recorded from $LaFeO_3$ (Fig. 2a) was composed of a sextet pattern similar to that reported earlier [15] with parameters $\delta = 0.36\,\mathrm{mm\,s^{-1}}$, $2\varepsilon = -0.09\,\mathrm{mm\,s^{-1}}$, $H = 52.7\,\mathrm{T}$ and $\Gamma = 0.32\,\mathrm{mm\,s^{-1}}$. The spectrum recorded following treatment in 10% hydrogen/90% nitrogen at 600°C (the first peak in the tpr profile) showed the partial reduction of the perovskite-related $LaFeO_3$ phase to metallic iron (Fig. 2b). The intensity of the sextet characteristic of metallic iron amounted to ca. 16% of

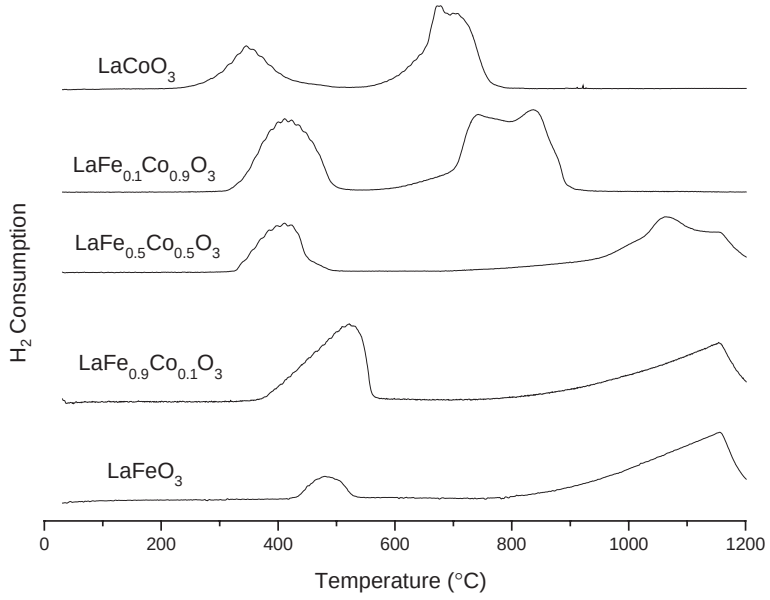

Fig. 1. Temperature programmed reduction profiles recorded from compounds of the type $LaFe_{1-x}Co_xO_3$.

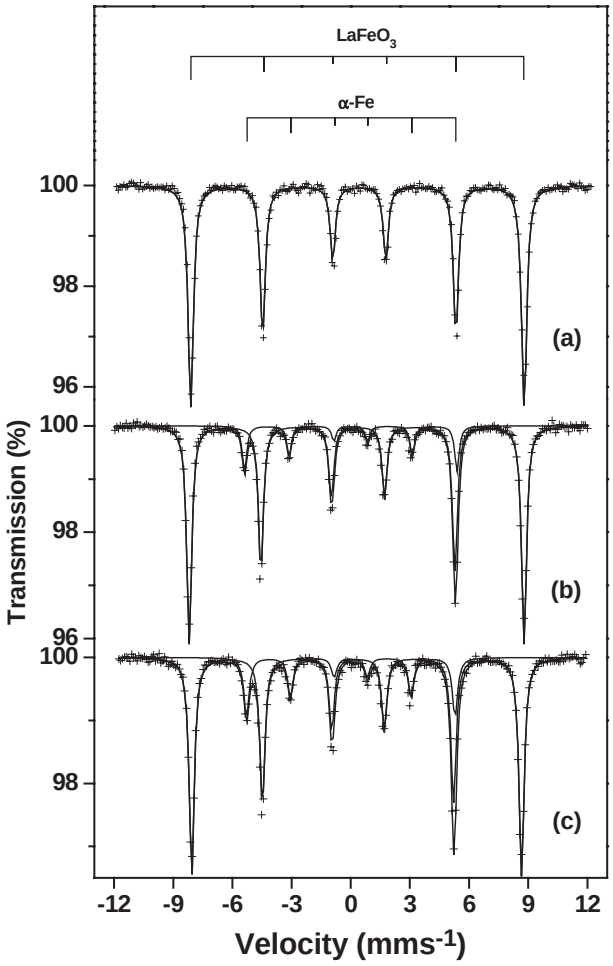

Fig. 2. ^{57}Fe Mössbauer spectra recorded at 298 K from (a) $LaFeO_3$ and following reduction at (b) 600°C and (c) 1200°C.

the spectral area. The spectrum recorded following treatment in the hydrogen/nitrogen gas mixture at 1200°C (after the second peak in the tpr profile) (Fig. 2c) showed an enhanced amount of metallic iron (ca. 22%) but without complete reduction of lanthanum orthoferrite.

The Fe K-edge XANES and EXAFS results are in good agreement with the ^{57}Fe Mössbauer data. The shape of the Fe K-edge XANES recorded from $LaFeO_3$ (Fig. 3(i) a) was similar to that reported previously [16]. The position of the edge at 7126.0 eV and the position of the edge crest at 7130.4 eV are characteristic of the presence of trivalent iron [17]. The Fe K-edge XANES recorded from the samples following treatment in hydrogen and nitrogen (Fig. 3(i) b and c) showed the presence of a feature at ca. 7114.2 eV which is close to the first inflexion point of the absorption edge of metallic iron. The intensity of this feature increases with increasing temperature treatment. This is consistent with the ^{57}Fe Mössbauer spectroscopy results and is indicative that the extent of reduction to metallic iron increases with treatment under reducing conditions at increasing temperatures. The existence of an increasing contribution of metallic iron is more clearly seen in the first derivative of the absorption edge (Fig. 3(i) a′–c′) which clearly shows changes in the region 7105–7115 (particularly the appearance of a maximum at 7112.4 eV which we associate with the presence of metallic iron).

The Fe K-edge EXAFS recorded from $LaFeO_3$ (Fig. 4(i)) were fitted according to the previously reported diffraction data [18] (Table 1). The results are in good agreement with this model, the Fe K-edge EXAFS being dominated by a first coordination shell of 6 oxygen atoms at 1.98 Å (Fig. 4(ii) a) which, given the XANES data, is consistent with an octahedrally coordinated Fe^{3+} species. The changes brought about by treatment in hydrogen and nitrogen are best appreciated by consideration of the Fe K-edge EXAFS (and the corresponding Fourier transform) recorded from the sample treated at 1200°C (Fig. 4(i) c) which clearly showed a contribution from metallic iron (Fe–Fe distance at 2.47 Å (Fig. 4(ii) c)) together with the $LaFeO_3$ contribution characterized by an Fe–O distance in the first coordination shell of 1.99 Å. The Fe^{3+}/Fe^0 ratio can be calculated from the ratio of the coordination numbers associated with the respective Fe–O and Fe–Fe distances. Since a strong correlation exists between the coordination numbers and Debye-Waller factors, the Debye-Waller factors were initially refined simultaneously. The Debye-Waller factors were then fixed to the nearest half-integer value and the coordination numbers were allowed to refine. Using this fitting procedure we obtained a Fe^{3+}/Fe^0 ratio of ca. 2.4 for the material treated at 1200°C in the hydrogen and nitrogen mixture. This demonstrates that ca. 31% of the total iron-containing phases in the material is composed of metallic iron. Given the inherent difficulty in determining coordination numbers by EXAFS, which can be affected by a large error [19], the results obtained from EXAFS are in acceptable agreement with those obtained from Mössbauer spectroscopy. The shells at ca. 3–3.5 Å correspond to Fe–La distances in the $LaFeO_3$ structure [18].

The La L_{III}-edge XANES (Fig. 3(ii)) were similar to those recorded from La_2O_3 and were compatible with the presence of La^{3+}. The La L_{III}-edge EXAFS (Figs. 4(iii) and (iv)) were successfully fitted (Table 1) to a first shell of 12 oxygen atoms according to the previously reported structural information [18] deduced from diffraction data. An important feature of the La L_{III}-edge XANES and EXAFS recorded from $LaFeO_3$ following treatment in the hydrogen/nitrogen gas mixture is their similarity to the data recorded from the original material (Figs. 3(ii)a–c and 4(iii) and (iv) a–c) indicative of the resistance of the trivalent lanthanum ion to a change in oxidation state or local coordination in the gaseous reducing atmosphere. Hence the results

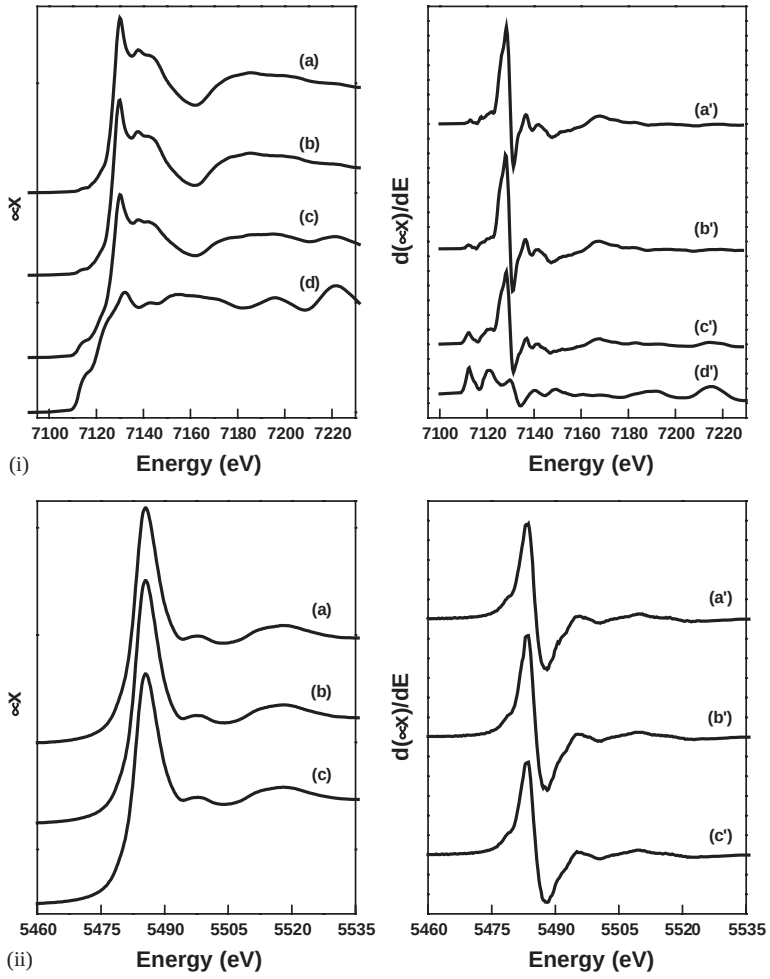

Fig. 3. (i) Fe K-edge- and (ii) La L_{III}-edge XANES recorded from (a) $LaFeO_3$ and following treatment in a hydrogen/nitrogen gas mixture at (b) 600°C and (c) 1200°C. (a′), (b′) and (c′) are the first derivative of (a), (b) and (c), respectively. The spectrum presented in (i) (d) corresponds to iron metal, (d′) is the first derivative of (d).

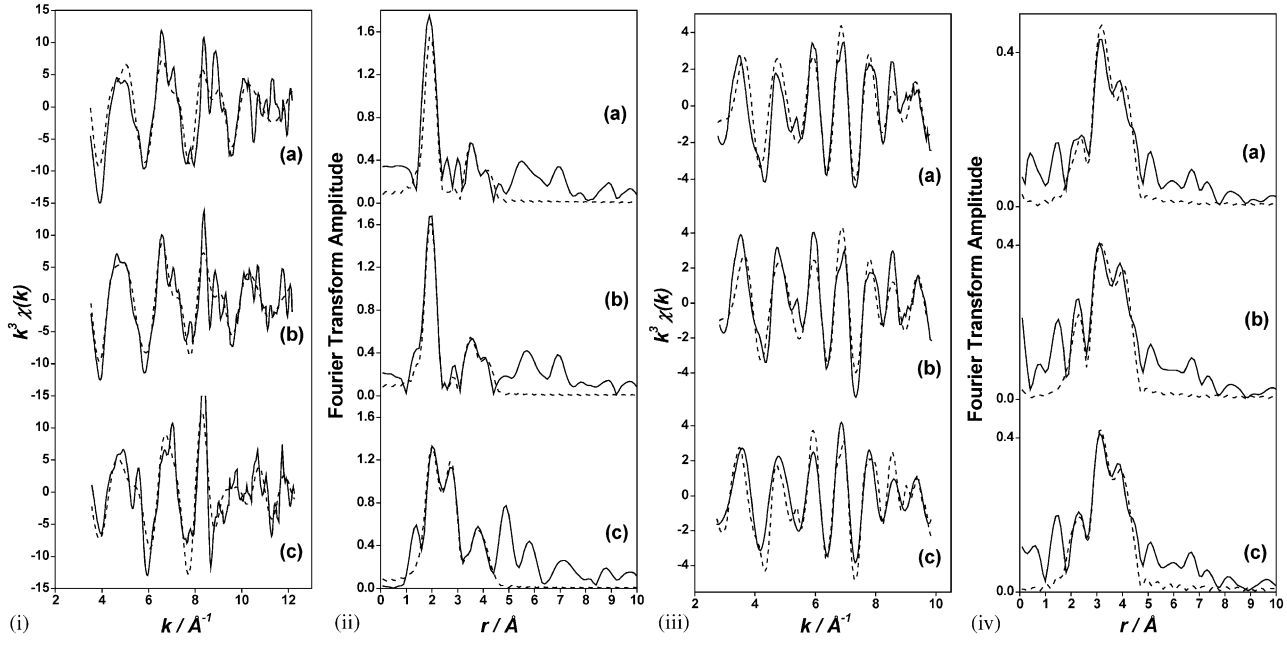

Table 1
Best fit parameters to the Fe K-edge and La L_{III}-edge EXAFS data recorded from $LaFeO_3$

	Diffraction data [18], coordination number [atom type] and distance (Å)	Initial model for EXAFS Coordination number [atom type] and distance (Å)	Best fit parameters		
			Coordination number and [atom type]	d (Å) ($\pm$0.02)	$2\sigma^2$(Å^2)
Fe K-edge	6[O]2.00,2[La]3.28,2[La]3.39, 2[La]3.43,2[La]3.54,6[Fe] 3.54	6[O]2.00 8[La]3.41 6[Fe]3.93	6[O] 8[La] 6[Fe]	1.98 3.30 4.00	0.010 0.032 0.026
La L_{III}-edge	1[O]2.44,2[O]2.46,1[O]2.59, 1[O]2.65,2[O]2.80,1[O]3.03, 1[O]3.14,2[O]3.27,2[Fe]3.28, 2[Fe]3.39,2[Fe]3.43,2[Fe]3.54, 2[La]3.88, 2[La]3.94, 2[La]3.98	3[O]2.46 6[O]2.76 3[O]3.22 2[Fe]3.28 6[Fe]3.45 6[La]3.94	3[O] 6[O] 3[O] 2[Fe] 6[Fe] 6[La]	2.47 2.71 3.27 3.36 3.43 3.90	0.032 0.050 0.006 0.029 0.042 0.023

imply that treatment of $LaFeO_3$ in the hydrogen/nitrogen gas mixture results in partial reduction of Fe^{3+} which segregates from the structure to form metallic iron but without collapse of the perovskite-related structure and/or the reduction and segregation of lanthanum-containing phases.

3.2. $LaFe_{0.9}Co_{0.1}O_3$

The ^{57}Fe Mössbauer spectrum recorded from $LaFe_{0.9}Co_{0.1}O_3$ (Fig. 5a) was similar to that of $LaFeO_3$ ($\delta = 0.36\,mm\,s^{-1}$, $2\varepsilon = -0.09\,mm\,s^{-1}$, $H = 51.5\,T$ and $\Gamma = 0.46\,mm\,s^{-1}$). The broader linewidth may reflect the introduction of cobalt into the cationic sublattice. The spectrum recorded after the first peak in the tpr profile (Fig. 5b) showed, besides the oxide contribution, an additional sextet with parameters ($\delta = 0.05\,mm\,s^{-1}$, $2\varepsilon = 0.00\,mm\,s^{-1}$, $H = 36.1\,T$) that are compatible with the presence of ca. 10% Fe–Co alloy [20]. The results indicate that the Fe^{3+} and Co^{3+} in $LaFe_{0.9}Co_{0.1}O_3$ are partially reduced and form an alloy. The ^{57}Fe Mössbauer spectrum recorded after the second reduction peak (Fig. 5c) showed the coexistence of metallic iron, an Fe–Co alloy, and the $LaFe_{0.9}Co_{0.1}O_3$ phase, with relative spectral areas of 16%, 19% and 65%, respectively. The result contrasts with that recorded from $LaFeO_3$ under reducing conditions in that the presence of cobalt appears to induce a greater degree of reduction, the segregation of both iron and cobalt and the formation of metallic and alloy phases. It is interesting to note the stability of $LaFeO_3$ and $LaFe_{0.9}Co_{0.1}O_3$ to reduction in the hydrogen/nitrogen gas mixture at 1200°C and that under these conditions reduction does not lead to destruction of the oxide structure.

3.3. $LaFe_{0.5}Co_{0.5}O_3$

The ^{57}Fe Mössbauer spectrum recorded at room temperature from $LaFe_{0.5}Co_{0.5}O_3$ (Fig. 6a) was very different from those recorded from $LaFeO_3$ and $LaFe_{0.9}Co_{0.1}O_3$. The spectrum showed a broad distribution of magnetic hyperfine fields characteristic of a system experiencing magnetic relaxation in the vicinity of a magnetic transition temperature. The isomer shift, quadrupole splitting and average magnetic hyperfine field obtained from the fit were $0.36\,mm\,s^{-1}$, $-0.003\,mm\,s^{-1}$ and 26.3 T, respectively. It seems that the substitution of 50% of the Fe^{3+} ions in $LaFeO_3$ by Co^{3+} induces a noticeable decrease in the magnetic ordering temperature. This was confirmed in the spectrum recorded at 80 K (Fig. 6b) from the same material which showed a well defined magnetic hyperfine pattern but with broadened linewidths and lower (49.7 T) average magnetic hyperfine field as compared with $LaFeO_3$ at room temperature. The spectrum recorded at 10 K showed a sextet pattern with relatively broad lines and a magnetic hyperfine field of 51.1 T (Fig. 6c).

The ^{57}Fe Mössbauer spectrum (Fig. 7b) recorded at 298 K from $LaFe_{0.5}Co_{0.5}O_3$ after the first reduction peak in the tpr profile (Fig. 1) also showed a distribution of

Fig. 4. (i) Fe K-edge-EXAFS (raw data) recorded from (a) $LaFeO_3$ and following treatment in a hydrogen/nitrogen gas mixture at (b) 600°C and (c) 1200°C; (ii) Fourier transforms of the EXAFS data presented in (i); (iii) La L_{III}-edge EXAFS recorded from (a) $LaFeO_3$ and following treatment in a hydrogen/nitrogen gas mixture at (b) 600°C and (c) 1200°C; (iv) Fourier transforms of the EXAFS data presented in (iii) (the experimental data are indicated by the solid line, the fits to the data are indicated by the broken line).

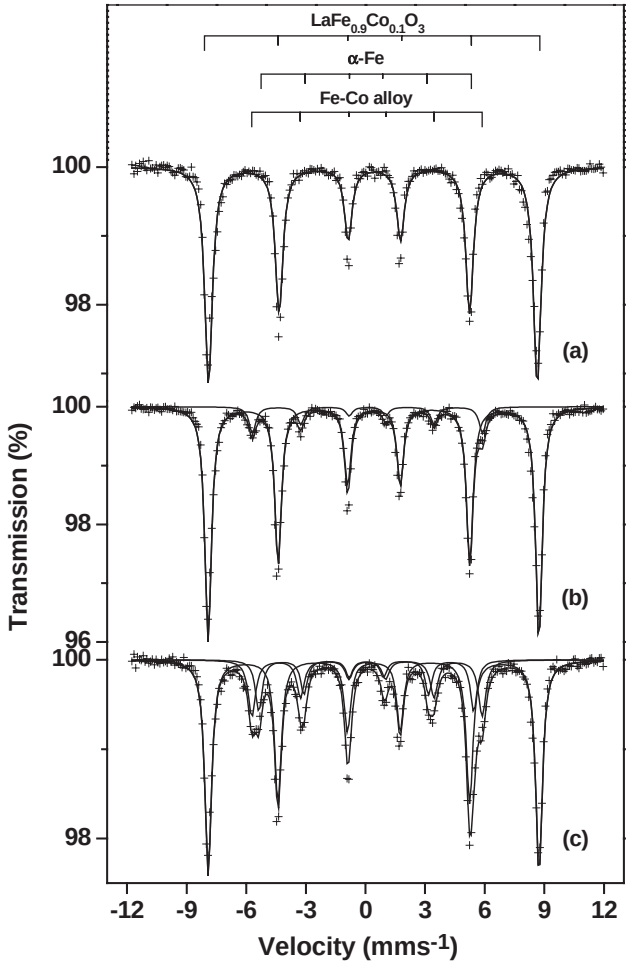

Fig. 5. ^{57}Fe Mössbauer spectra recorded at 298 K from (a) $LaFe_{0.9}Co_{0.1}O_3$ and following reduction at (b) 600°C and (c) 1200°C.

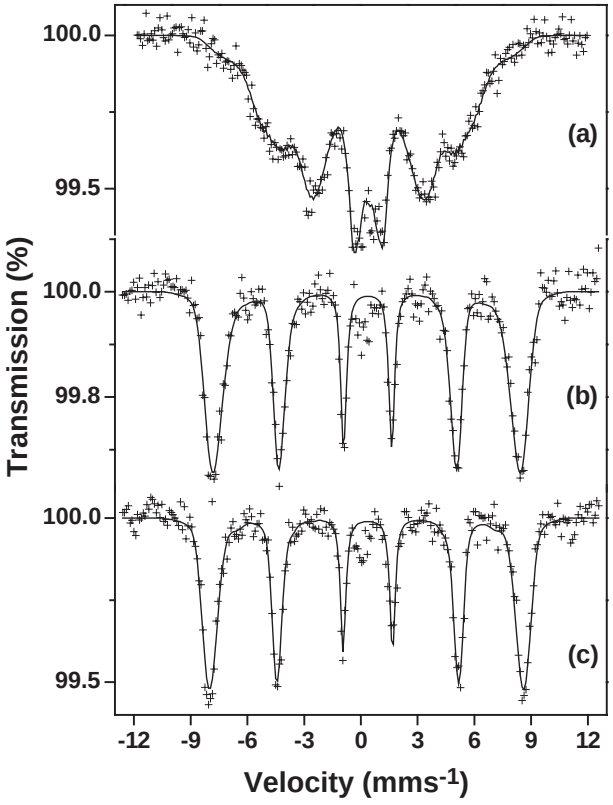

Fig. 6. ^{57}Fe Mössbauer spectra recorded at 298, 80 and 10 K from $LaFe_{0.5}Co_{0.5}O_3$.

magnetic hyperfine fields. The broadness of the spectral lines and poor statistics precluded the identification of a component corresponding to metallic iron. Whether or not iron and/or cobalt segregate from the material during the initial treatment in the reducing atmosphere is therefore unclear on the basis of Mössbauer spectroscopy data alone.

The ^{57}Fe Mössbauer spectrum recorded from materials following treatment in the hydrogen/nitrogen mixture at 1000°C (Fig. 7c) showed a sextet pattern (accounting for ca. 53% of the spectral area) with similar parameters to those of $LaFeO_3$ together with another broad sextet which was deconvoluted into two sextets: one characteristic of metallic iron ($\delta = 0.00\,\mathrm{mm\,s^{-1}}$, $2\varepsilon = 0.00\,\mathrm{mm\,s^{-1}}$ and $H = 33.0\,\mathrm{T}$ Area=6%) and a second more intense component (ca. 41%) with Mössbauer parameters $\delta = 0.04\,\mathrm{mm\,s^{-1}}$, $2\varepsilon = -0.04\,\mathrm{mm\,s^{-1}}$ and $H = 34.8\,\mathrm{T}$ which are compatible with the presence of an iron–cobalt alloy [20]. The result indicates that treatment under reducing conditions at 1000°C induces the partial segregation of iron and cobalt from the perovskite-related oxide structure and the formation of metallic and alloy phases but without total destruction of the perovskite-related structure. The spectrum recorded from the material following further treatment in the hydrogen/nitrogen gas mixture at 1200°C (Fig. 7d) did not show any sextet component with isomer shift values which could be associated with an oxide species. It consisted of a sextet containing contributions from both metallic iron (ca. 33%) and iron–cobalt alloy (ca. 67%). The magnetic hyperfine field obtained from the fit of the spectrum to the iron–cobalt alloy (35.7 T) was slightly higher than that observed in the case of the material formed at 1000°C indicating that the composition of this phase could be slightly different. The results demonstrate that in this material the Fe^{3+} and Co^{3+} ions in the perovskite-related structure are more susceptible to reduction than in the material of composition $LaFeO_3$ and, at the higher temperatures, their segregation to form metallic and alloy phases is accompanied by the collapse of the oxide structure.

The Fe K-edge XANES recorded from $LaFe_{0.5}Co_{0.5}O_3$ before and after tpr treatment are in good agreement with the Mössbauer data. The Fe K-edge XANES recorded from $LaFe_{0.5}Co_{0.5}O_3$ (Fig. 8(i) a) is similar to that recorded from $LaFeO_3$ (position of the absorption edge 7126.0 eV) and are consistent with the presence of an Fe^{3+}-containing species. The Fe K-edge

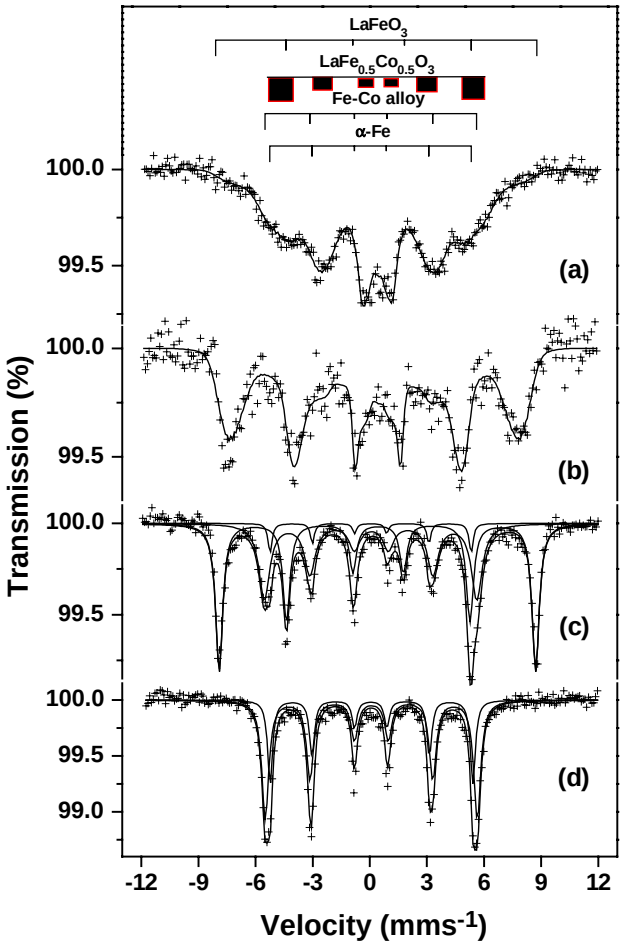

Fig. 7. ^{57}Fe Mössbauer spectra recorded at 298 K from (a) $LaFe_{0.5}Co_{0.5}O_3$ and following reduction at (b) 500°C, (c) 1000°C, and (d) 1200°C.

XANES recorded from the material treated at 500°C in the hydrogen/nitrogen gas mixture (Fig. 8(i) b) (i.e., after the first peak in the tpr profile, Fig. 1) is also similar. However, close inspection of the first derivative of the absorption edge recorded from this sample (Fig. 8(i) b′) shows some small change in the region 7105–7115 eV that could be compatible with the presence of a small amount of Fe^0. The Fe K-absorption edge recorded from the material following treatment in hydrogen and nitrogen at 1000°C (Fig. 8(i) c) shows the presence of a feature at ca. 7114.3 eV suggestive of the presence of Fe^0. Inspection of the first derivative of the absorption edge recorded from this material showed (Fig. 8(i) c′) that, although there are some oscillations compatible with the presence of Fe^{3+} within the perovskite-related structure, a considerable contribution from iron in the Fe^0 state is also present. Taken in conjunction with the Mössbauer spectroscopy data the results confirm the reduction of Fe^{3+} in the perovskite-related structure and the formation of metallic iron and the iron–cobalt alloy. The absorption edge in the Fe K-edge XANES recorded from the material treated at 1200°C appears at 7112.4 eV (Fig. 8(i) d). The position and shape of the edge features are compatible with the exclusive presence of Fe^0. It is interesting to note the characteristic maxima appearing in the first derivative of the absorption edge between 7105 and 7115 eV which lends support to the probability of Fe^0 in the spectra of the samples treated in hydrogen and nitrogen at 500°C. The results clearly indicate that all the Fe^{3+} ions present in the original material are reduced to Fe^0 at 1200°C in the reducing atmosphere and are consistent with the Mössbauer spectroscopy data.

The changes brought about by the tpr treatment are also well illustrated by the Fe K-edge EXAFS and their respective Fourier transforms (Figs. 9(i) and (ii)). The data recorded from pure $LaFe_{0.5}Co_{0.5}O_3$ (Table 2) were best fitted to a similar model to that used to fit the Fe K-edge EXAFS recorded from $LaFeO_3$. The shape and frequency of the EXAFS oscillations recorded from the material treated at 500°C (Fig. 9(i) b) are very similar to those of the original material. Consequently, the parameters obtained from the fit were also very similar. The small contribution from Fe^0 suggested by the XANES results appear not to be clearly reflected in the corresponding EXAFS. Indeed, attempts to fit the data with a contribution from Fe^0 did not significantly improve the goodness of the fit. The result implies that the extent of any reduction of iron is, at best, small. The Fe K-edge EXAFS recorded from the material following treatment in hydrogen and nitrogen at 1000°C (Fig. 9(i) c) showed in the first coordination shell, in addition to the Fe–O distance of 1.97 Å characteristic of Fe^{3+} in the perovskite structure, an important contribution due to a Fe–Fe/Co distance at 2.45 Å and a new Fe–Fe/Co shell at ca. 4.5 Å (Fig. 9(ii) c). We associate these with the presence of Fe^0 as shown by XANES and Mössbauer spectroscopy. We would mention that it is difficult to distinguish between Fe–Fe and Fe–Co distances by EXAFS since the atomic radii of iron and cobalt are very similar. In this sense, Mössbauer spectroscopy appears to be a more sensitive technique to identify both the bcc α-Fe from the bcc α-Fe–Co alloy. The Fe-K-edge EXAFS recorded from the material treated at 1200°C (Fig. 9(i) d and Table 2) was characteristic of a metallic phase and confirms the results shown by Mössbauer spectroscopy and XANES that treatment under reducing conditions at 1200°C brings about the complete reduction of Fe^{3+} to Fe^0 and the formation of metallic iron and an iron–cobalt alloy.

The Co K-edge XANES and EXAFS showed interesting trends. The position of the edge of the Co K-edge XANES recorded from $LaFe_{0.5}Co_{0.5}O_3$ at 7723.3 eV (Fig. 8(ii) a and a′) is close to that reported previously for $LaCoO_3$ [21] and confirms that cobalt is in the trivalent state in this material. The Co K-edge XANES recorded from the material following treatment in hydrogen/nitrogen at 500°C showed (Fig. 8(ii) b and b′)

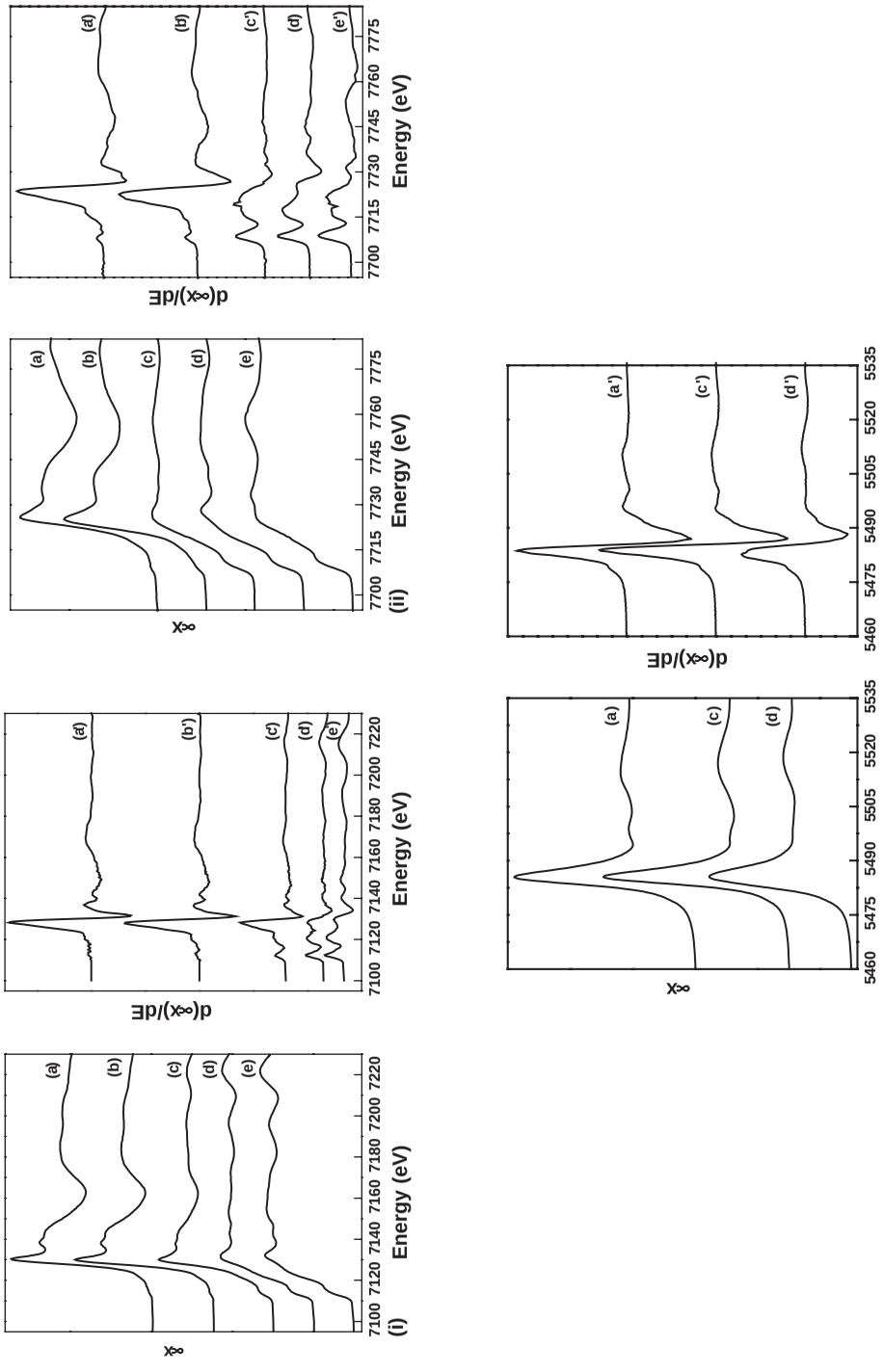

Fig. 8. (i) Fe K-edge, (ii) Co K-edge, and (iii) La L_{III}-edge- XANES recorded from (a) $LaFe_{0.5}Co_{0.5}O_3$ and following treatment in a hydrogen/nitrogen gas mixture at (b) 500°C, (c) 1000°C and (d) 1200°C. (a′), (b′), (c′) and (d′) are the corresponding first derivative spectra of (a), (b), (c) and (d). The spectra presented in (i) (e) and (ii) (e) correspond to iron metal and cobalt metal, respectively; (e′) is the corresponding first derivative of (e).

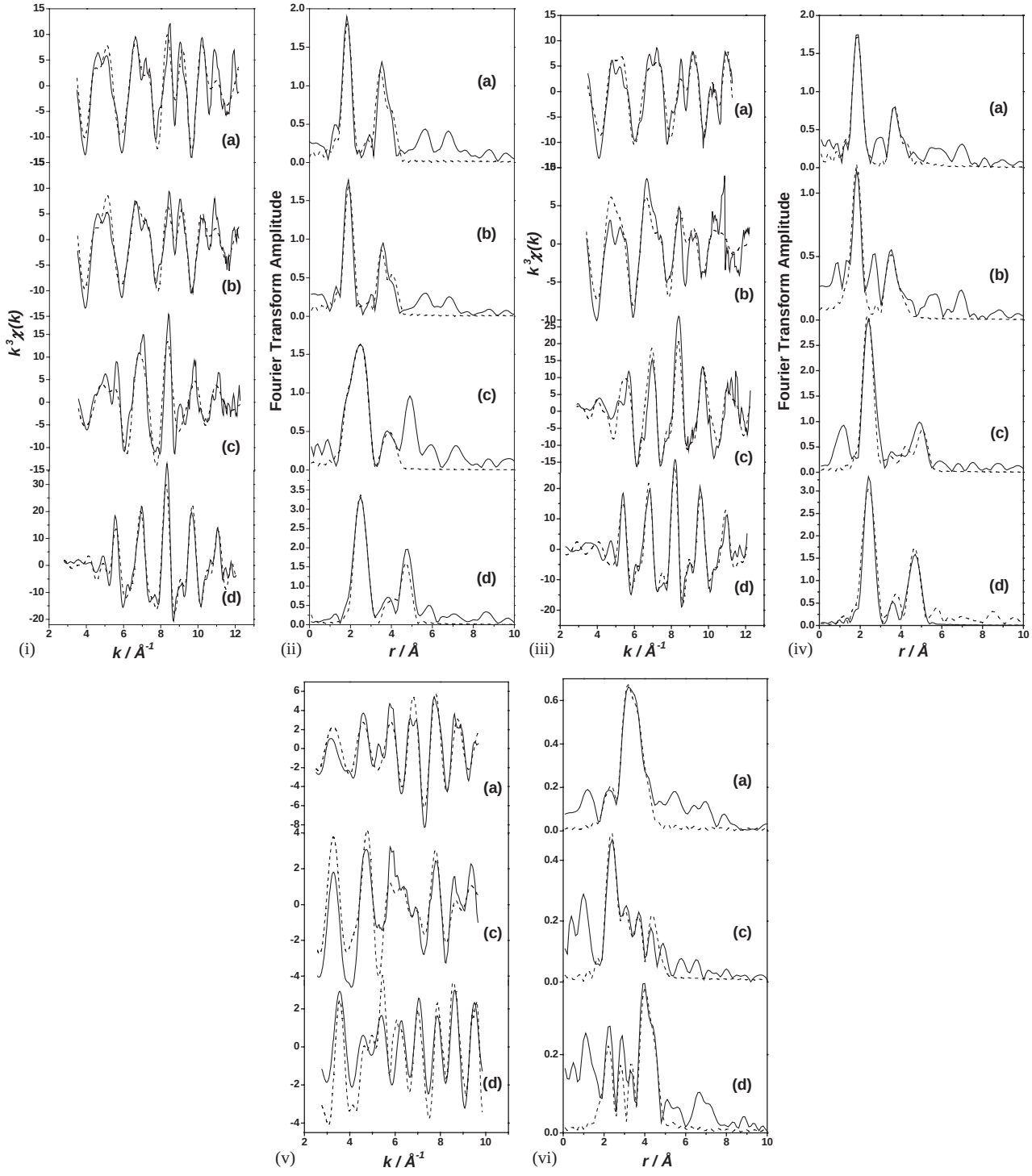

Fig. 9. (i) Fe K-edge EXAFS (raw data) recorded from $LaFe_{0.5}Co_{0.5}O_3$ (a) and following treatment in a hydrogen/nitrogen gas mixture at (b) 500°C, (c) 1000°C, and (d) 1200°C; (ii) Fourier transforms of the EXAFS data presented in (i); (iii) Co K-edge EXAFS (raw data) recorded from $LaFe_{0.5}Co_{0.5}O_3$ (a) and following treatment in a hydrogen/nitrogen gas mixture at (b) 500°C, (c) 1000, and (d) 1200°C; (iv) Fourier transforms of the EXAFS data presented in (iii); (v) La L_{III}-edge EXAFS recorded from $LaFe_{0.5}Co_{0.5}O_3$ (a) and following treatment in a hydrogen/nitrogen gas mixture at (c) 1000°C and (d) 1200°C; (vi) Fourier transforms of the EXAFS data presented in (v) (the experimental data are indicated by the solid line, the fits to the data are indicated by the broken line).

small changes in the region 7704–7714 eV. Given that the position of the first inflection point on the cobalt foil edge was at 7708.9 eV the result is compatible with the partial reduction of Co^{3+} to Co^0. The first maximum in the first derivative of the Co K-edge recorded from the material after treatment at 1000 and 1200°C in hydrogen

Table 2
Best fit parameters to the Fe K-edge, Co K-edge and La L_{III}-edge EXAFS recorded from $LaFe_{0.5}Co_{0.5}O_3$ and following treatment in hydrogen and nitrogen at 1200°C

	$LaFe_{0.5}Co_{0.5}O_3$			$LaFe_{0.5}Co_{0.5}O_3$ treated at 1200°C in hydrogen and nitrogen		
	Coordination number and [atom type]	d (Å) ($\pm$0.02)	$2\sigma_2$ (Å^2)	Coordination number and [atom type]	d (Å) ($\pm$0.02)	$2\sigma^2$ (Å^2)
Fe K-edge	6[O]	1.98	0.008	8[Fe/Co]	2.48	0.014
	8[La]	3.30	0.020	6[Fe]	2.83	0.020
	6[O]	3.97	0.014	12[Fe]	4.03	0.024
Co K-edge	6[O]	1.91	0.010	9[Fe/Co]	2.45	0.016
	8[La]	3.29	0.044	6[Fe/Co]	3.48	0.036
	6[Fe/Co]	3.93	0.004	9[Fe/Co]	4.30	0.024
La L_{III}-edge	3[O]	2.52	0.015	4[O]	2.43	0.028
	6[O]	2.76	0.018	3[O]	2.70	0.019
	3[O]	2.96	0.011	12[La]	3.85	0.036
	8[Fe]	3.39	0.022	6[La]	4.20	0.027

and nitrogen (Fig. 8(ii) c′ and d′) and corresponding to the third and forth peak in the tpr profile (Fig. 1) occurs at 7708.4 eV, a value that corresponds to the position of the first maximum in the first derivative of the XANES recorded from metallic cobalt. Inspection of the first derivative of the absorption edge (Fig. 8(ii) c′ and d′) also shows that differences occur in the local structure around cobalt in the samples treated at 1000°C and 1200°C in hydrogen and nitrogen. Thus, we associate this with the coexistence of Fe–Co alloy and metallic cobalt phases but with different concentrations in each sample. It is interesting to note that while there exists an oxide contribution in both the Mössbauer spectra and Fe K-edge XANES in the sample treated at 1000°C in hydrogen and nitrogen, the Co K-edge XANES data show only Co^0 contributions. Hence, at 1000°C, all the Co^{3+} is reduced to Co^0 while a significant fraction of iron remains present as Fe^{3+}.

The Co–O distances obtained by fitting of the Co K-edge EXAFS recorded from $LaFe_{0.5}Co_{0.5}O_3$ (Figs. 9(iii) and (iv) and Table 2) are in excellent agreement with the EXAFS data recently reported on compounds of related composition [21]. Although analysis of the Co K-edge EXAFS recorded from these samples heated in hydrogen and nitrogen at 500°C may show the presence of a small amount of Co^0, the data (Fig. 9(iii) b and Table 2) unequivocally indicate the presence of only Co^0 in the material treated in hydrogen and nitrogen at 1000°C and 1200°C and thereby endorse the evidence from XANES for the exclusive presence of Co^0 in these materials.

The position of the La L_{III}-edge recorded from $LaFe_{0.5}Co_{0.5}O_3$ (Fig. 8(iii) a) was similar to that recorded from $LaFeO_3$ (Fig. 3(ii) a). The position of the absorption edge did not change in samples following treatment in hydrogen and nitrogen and indicates that there is no reduction of La^{3+} although the attenuation of the small peak at ca. 5500 eV (Fig. 8(iii) a–c) as well as the increasing broadness of the white line as the temperature of reduction increases suggests changes in the local environment of lanthanum. These changes are better appreciated by a consideration of the La L_{III}-edge EXAFS recorded from these samples (Figs. 9(v) and (vi)). The La L_{III}-edge EXAFS recorded from $LaFe_{0.5}Co_{0.5}O_3$ was fitted on the basis of recent EXAFS analysis of $LaCoO_3$ [22]. The results are presented in Table 2. The Fourier transform of the EXAFS recorded from the sample treated in hydrogen and nitrogen at 1000°C shows (Fig. 9(vi) c) the disruption of the shell at 3–4.5 Å which is characteristic of the perovskite phase [22], the EXAFS being dominated by a first shell corresponding to La–O distances (Fig. 9(vi) c). The La L_{III}-edge EXAFS recorded from materials treated at 1200°C gave very different EXAFS (Fig. 9(v) d). The fit of these data (Table 2) is in excellent agreement with the presence of La_2O_3 [23]. Summarizing, it seems that for the material of composition $LaFe_{0.5}Co_{0.5}O_3$ the tpr treatment induces first the reduction of Co^{3+} and Fe^{3+} to form an Fe–Co alloy as well as metallic cobalt and metallic iron phases. The complete reduction of Co^{3+} occurs at lower temperature than the complete reduction of Fe^{3+}. The alloy- and metallic-phases segregate with the concomitant destruction of the perovskite structure and the formation of La_2O_3.

3.4. $LaFe_{0.1}Co_{0.9}O_3$

The ^{57}Fe Mössbauer spectrum recorded from $LaFe_{0.1}Co_{0.9}O_3$ (Fig. 10a) was composed of a single peak ($\delta = 0.36\,mm\,s^{-1}$) demonstrating that the substitution of

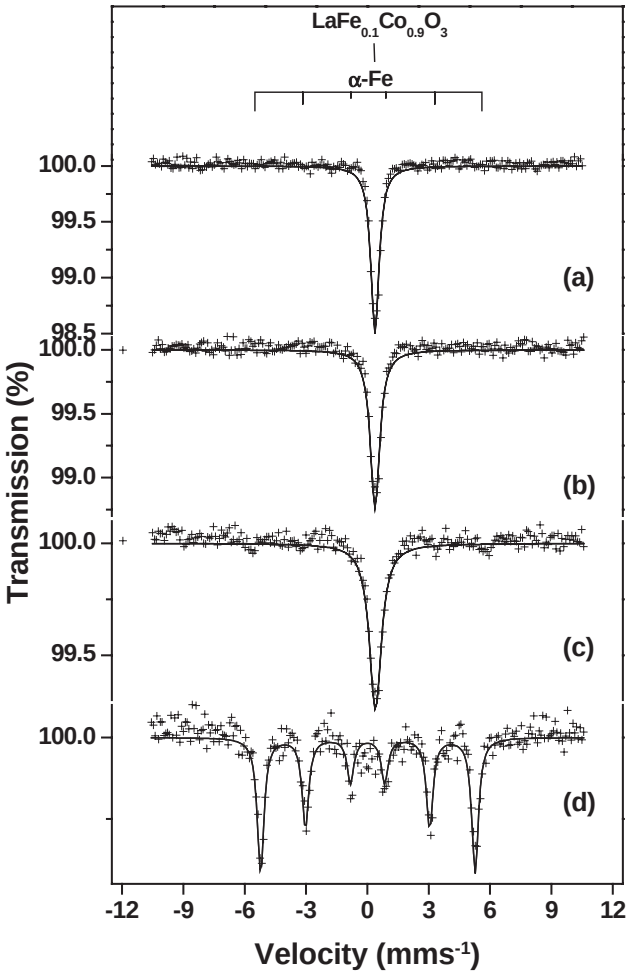

Fig. 10. ^{57}Fe Mössbauer spectra recorded from (a) $LaFe_{0.1}Co_{0.9}O_3$ and following reduction at (b) 500°C, (c) 800°C, and (d) 900°C.

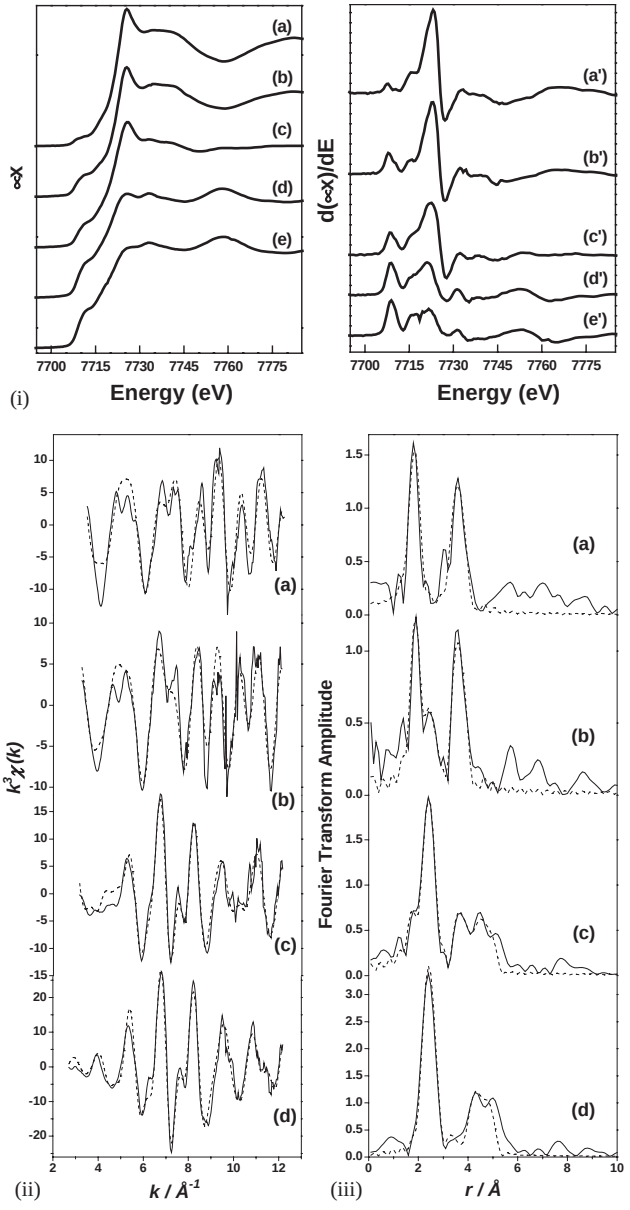

Fig. 11. (i) Co K-edge XANES recorded from (a) $LaFe_{0.1}Co_{0.9}O_3$ and following treatment in a hydrogen/nitrogen gas mixture at (b) 500°C, (c) 800°C, and (d) 900°C; (a′), (b′), (c′) and (d′) are the first derivative spectra of (a), (b), (c) and (d), respectively. The spectrum presented in (i) (e) corresponds to cobalt metal and (e′) is the corresponding first derivative of (e). (ii) Co K-edge EXAFS recorded from (a) $LaFe_{0.1}Co_{0.9}O_3$ and following treatment in a hydrogen/nitrogen gas mixture at (b) 500°C, (c) 800°C and (d) 900°C. (iii) Fourier transforms (the experimental data are indicated by the solid line, the fits to the data are indicated by the broken line).

90% of the Fe^{3+} by Co^{3+} ions induces the total collapse of the magnetic interactions at room temperature. The dilution of the magnetic interactions induced by the presence of Co^{3+} is noticeably strong since the Mössbauer spectra continued to show a paramagnetic singlet component at temperatures as low as 12 K. The spectra recorded from the samples following treatment in hydrogen and nitrogen at 500°C and 800°C also showed a paramagnetic singlet (Fig. 10b and c). Treatment in the reducing gas mixture at 900°C gave complete reduction to metallic iron (Fig. 10d). Hence cobalt enhances the susceptibility to reduction of iron in the cobalt-rich $La(Fe/Co)O_3$ phases such that, at a low temperature of 900°C, metallic iron segregates from the structure.

The Co K-edge-XANES and EXAFS (Fig. 11) showed that ca. 10% of the Co^{3+} is reduced to Co^0 by treatment in hydrogen/nitrogen at 500°C and ca. 90% is reduced at 800°C. The La L_{III}-edge XANES and EXAFS indicated that the perovskite-related structure is largely destroyed by treatment in the reducing atmosphere at 800°C and that lanthanum exists in a complex oxide matrix which resisted identification by X-ray powder diffraction.

Hence, in the cobalt-rich $LaFe/CoO_3$ materials, treatment in the reducing gaseous atmosphere induces the facile reduction of iron and cobalt to the metallic

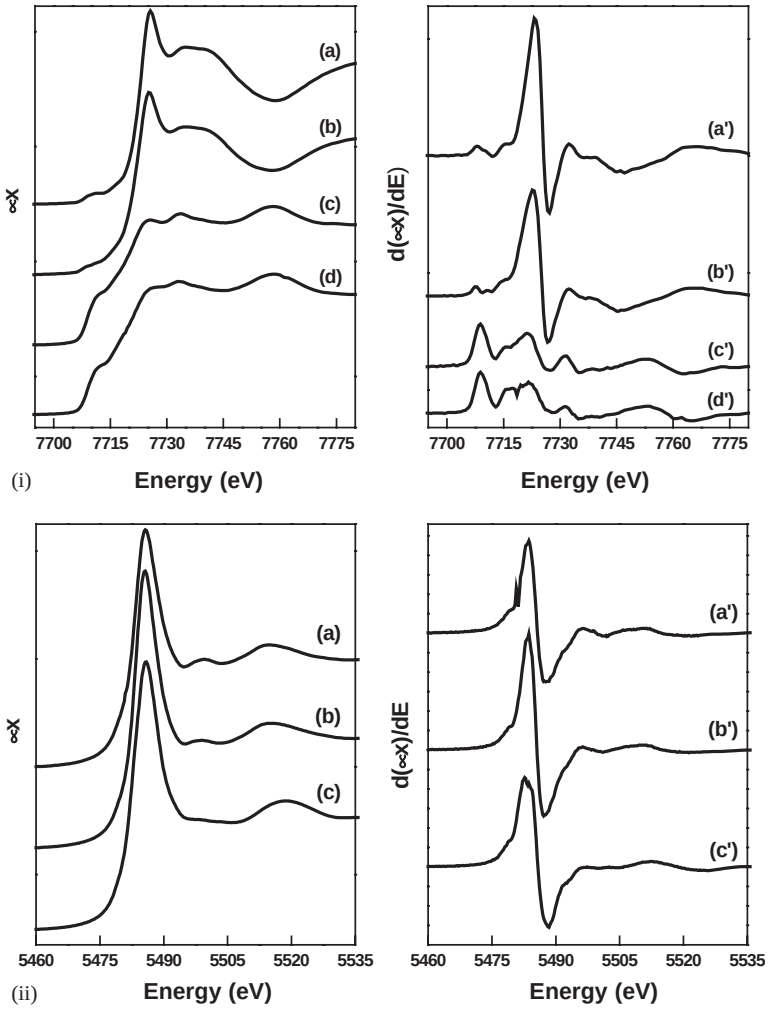

Fig. 12. (i) Co K-edge and (ii) La L_{III}-edge XANES recorded from (a) $LaCoO_3$ and following treatment in a hydrogen/nitrogen gas mixture at (b) 500°C and (c) 900°C. (a′), (b′) and (c′) are the first derivative of (a), (b) and (c), respectively. The spectrum presented in (i) (d) corresponds to cobalt metal and (d′) is the corresponding first derivative of (d).

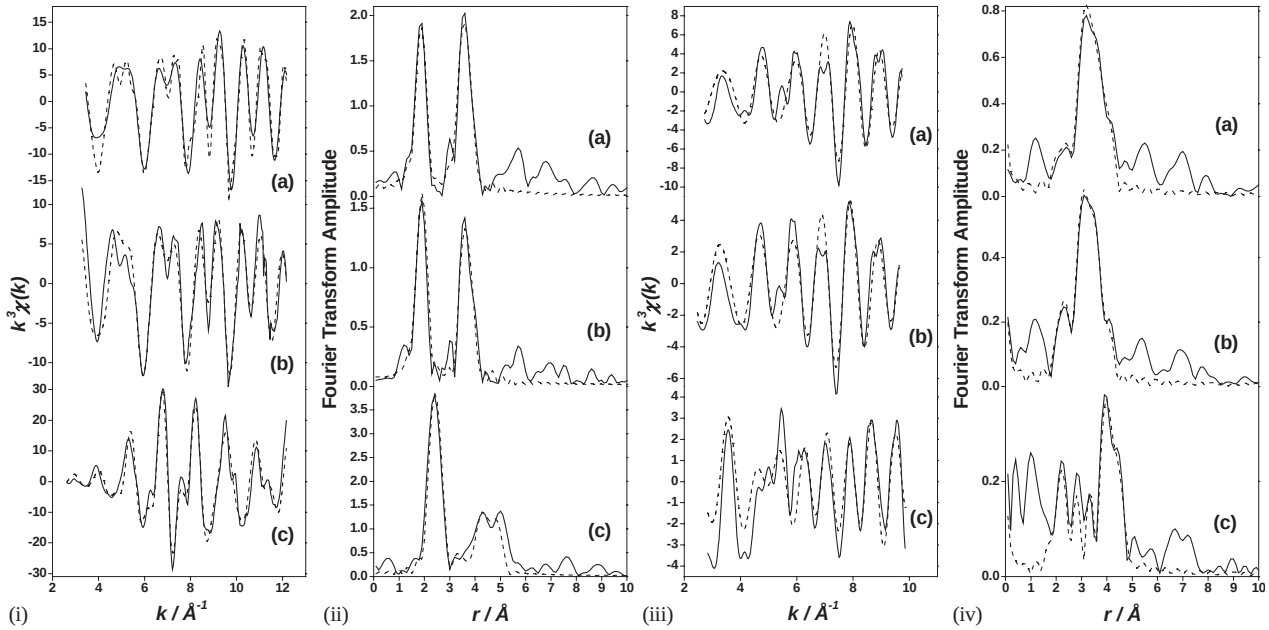

Table 3
Results of the fit of Co K-edge and La L_{III}-edge EXAFS recorded from $LaCoO_3$

	Literature values for $LaCoO_3$ [21]	$LaCoO_3$			$LaCoO_3$ treated at 900°C in hydrogen and nitrogen		
		Coordination number and [atom type]	d (Å) ($\pm$0.02)	$2\sigma^2$ (Å^2)	Coordination number and [atom type]	d (Å) ($\pm$0.02)	$2\sigma^2$ (Å^2)
Co K-edge	6[O]1.93	6[O]	1.92	0.009	9[Co]	2.49	
	8[La]3.30	8[La]	3.27	0.017	6[Co]	3.50	
	6[O]3.81	6[Co]	3.88	0.001	9[Co]	4.32	
La L_{III}-edge	3[O]2.43	3[O]	2.49	0.011	4[O]	2.43	0.029
	6[O]2.69	6[O]	2.72	0.016	3[O]	2.69	0.020
	3[O]3.00	3[O]	2.95	0.028	12[La]	3.84	0.036
	6[Co]3.31	6[Co]	3.32	0.019	6[La]	4.19	0.027
	6[La]3.81	6[La]	3.77	0.024			

states at temperatures exceeding ca. 800°C with simultaneous destruction of the perovskite lattice.

3.5. $LaCoO_3$

The Co K-edge XANES and EXAFS data (Figs. 12 and 13, Table 3) recorded from $LaCoO_3$ were similar to those recently reported [21]. The results recorded from the material following treatment in hydrogen and nitrogen at 500°C are very similar to the results recorded from the original materials except for a diminished amplitude of the EXAFS oscillations at both the Co K- and La L_{III}-edges. It seems that treatment at this temperature, rather than inducing the reduction of Co^{3+}, increases the extent of disorder in the materials. The data recorded from the materials following treatment at 900°C indicate the total reduction of Co^{3+} and the formation of metallic cobalt and La_2O_3 phases.

4. Conclusion

The incorporation of increasing concentrations of cobalt into materials of the type $LaFe_{1-x}Co_xO_3$ enhances the susceptibility of the materials to reduction in a hydrogen/nitrogen atmosphere. In materials with small cobalt concentrations ($x \leqslant$ ca. 0.1) reduction of trivalent iron and cobalt occurs to give metallic iron and iron–cobalt alloys without destruction of the perovskite structure even at elevated (ca. 1200°C) temperatures. In materials where $x \geqslant 0.5$ the reduction of Co^{3+} to Co^0 precedes complete reduction of Fe^{3+} and the segregation of alloy and metal and leads to concomitant destruction of the perovskite structure.

References

[1] C. Vasques, P. Kogerler, M.A. López-Quintela, J. Mater. Res. 13 (1998) 451.
[2] A.S. Moskvin, N.S. Ovanesyan, V.A. Trukhtarnov, Hyperfine Interactions 1 (1975) 265.
[3] J.G. McCarty, H. Wise, Catal. Today 8 (1990) 231.
[4] Y. Shimizu, M. Shimabukuro, H. Arai, T. Seiyama, Chem. Lett. (1985) 917.
[5] T. Arakawa, H. Kurachi, J. Shiokawa, J. Mater. Sci. 4 (1985) 1207.
[6] Y. Matsuura, S. Matsushima, M. Sakamoto, Y. Sadoaka, J. Mater. Chem. 3 (1993) 767.
[7] F.G. Karlsson, Electrochim. Acta 30 (1985) 1555.
[8] T. Nekamura, G. Petzow, L.J. Gancker, Mater. Res. Bull. 14 (1979) 649.
[9] J. Mizusaki, T. Sisamoto, W.K. Cannon, H.K. Bowen, J. Am. Ceram. Soc. 65 (1982) 363.
[10] Y. Sadaoka, E. Traversa, P. Nunziante, M. Sakamoto, J. Alloys Compd. 261 (1997) 182.
[11] E. Traversa, P. Nunziante, M. Sakamoto, Y. Sodoaka, R. Montanar, Mater Res. Bull. 33 (1998) 673.
[12] V.R. Choudhary, B.S. Uphade, S.G. Pataskar, Fuel 78 (1999) 919.
[13] Y. Nishihata, J. Mizuki, T. Akao, H. Tanaka, M. Uenishi, M. Kimura, T. Okamoto, N. Hamada, Nature 418 (2002) 164.
[14] W. Kraus, G. Nolze, Federal Institute for Materials Research and Testing, Berlin, Germany, 2000.
[15] M. Eibschitz, S. Shtrikmand, D. Treves, Phys. Rev. 156 (1967) 562.

Fig. 13. (i) Co K-edge EXAFS (raw data) recorded from (a) $LaCoO_3$ and following treatment in a hydrogen/nitrogen gas mixture at (b) 500°C and (c) 900°C; (ii) Fourier transforms of the EXAFS data presented in (i); (iii) La LIII-edge EXAFS recorded from (a) $LaCoO_3$ and following treatment in a hydrogen/nitrogen gas mixture at (b) 500°C and (c) 900°C; (iv) Fourier transforms of the EXAFS data presented in (iii) (the experimental data are indicated by the solid line, the fits to the data are indicated by the broken line).

[16] B. Buffat, M.H. Tuilier, Sol. State Commun. 64 (1987) 401.
[17] N. Binsted, G.N. Greaves, C.M.B. Henderson, J. Phys. Coll. C 8 12 (1986) C8-837.
[18] H. Falcon, A.E. Goeta, G. Punte, R.E. Carbonio, J. Solid State Chem. 133 (1997) 379.
[19] P. Eisenberger, B. Lengeler, Phys. Rev. 22 (1980) 3551.
[20] V. Carles, C. Laurent, M. Brieu, A. Rousset, J. Mater. Chem. 9 (1999) 1003.
[21] P. Porta, S. de Rossi, M. Faticanti, G. Minelli, I. Pettiti, L. Lisi, M. Turco, J. Solid State Chem. 146 (1999) 291.
[22] S. Colonna, S. de Rossi, M. Faticanti, I. Pettiti, L. Lisi, P. Porta, J. Mol. Catal A: Chem. 180 (2002) 161.
[23] F. Ali, A.V. Chadwick, M.E. Smith, J. Mater. Chem. 7 (1997) 285.